Inorg. Chem. **2007**, *46*, 1751−1759

Synthesis and Characterization of Copper(II) Complexes of Nonfacially Coordinating Heteroscorpionate Ligands (4-Carboxyphenyl)bis(3,5-dimethylpyrazolyl)methane and (3-Carboxyphenyl)bis(3,5-dimethylpyrazolyl)methane

Guillermo A. Santillan and Carl J. Carrano*

Department of Chemistry and Biochemistry, San Diego State University, San Diego, California 92182-1030

Received November 22, 2006

Complexes of Cu(II) derived from two new nonfacially coordinating heteroscorpionate ligands, (4-carboxyphenyl)-bis(3,5-dimethylpyrazolyl)methane (L4c) and (3-carboxyphenyl)bis(3,5-dimethylpyrazolyl)methane (L3c), have been synthesized and characterized by X-ray diffraction, ESI-MS, IR, and UV–vis spectroscopy, electrochemistry, and magnetic susceptibility. The use of these new complexes as building blocks for the construction of supramolecular architectures is discussed.

Introduction

The development of coordination polymers or metal−organic frameworks (MOF) is of great current interest because of their potential applications in a variety of different areas including molecular magnetism,[1−3] electronic conductivity,[4] host−guest chemistry,[5−8] sensors,[9] and optical devices.[10] These materials are constructed of metal centers connected through organic ligands that can lead to extended multidimensional topologies.[11,12] One approach for the rational design of such systems is through molecular self-assembly of simple building blocks and linkers.[13−16] Polytopic organic carboxylates and nitrogen heterocycles have been widely used as bridging motifs in the development of these metallosupramolecular complexes.[17−18] On the other hand nitrogen-, oxygen-, and sulfur-based multidentate scorpionate and heteroscorpionate ligands have been used almost exclusively as nonbridging, facially coordinating ligands designed to enforce mononuclearity.[19,20] Recently, however new bispyrazolyl derivatives and other scorpionate ligands have been developed to generate metallosupramolecular complexes.[21−25]

* To whom correspondence should be addressed. E-mail: carrano@sciences.sdsu.edu.

(1) Caneschi, A.; Gatteschi, D.; Lalioti, N.; Sengregorio, C. *Angew. Chem., Int. Ed.* **2001**, *40*, 1760−1763.
(2) Clerac, R.; Miyasaka, H.; Yamashita, M.; Coulon, C. *J. Am. Chem. Soc.* **2002**, *124*, 12837−12844.
(3) Ichikawa, S.; Kimura, S.; Mori, H.; Yoshida, G.; Tajima, H. *Inorg. Chem.* **2006**, *45*, 7575−7577.
(4) Kitagawa, H.; Onodera, N.; Sonoyama, T.; Yamamoto, M.; Fukawa, T.; Mitani, T.; Seto, M.; Maeda, Y. *J. Am. Chem. Soc.* **1999**, *121*, 10068−10080.
(5) Albrecht, M.; Janser, I.; Burk, S.; Weis, P. *Dalton Trans.* **2006**, 2875−2880.
(6) Seeber, G.; Tiedemann, B.; Raymond, K. N. *Top. Curr. Chem.* **2006**, *265*, 147−183.
(7) Leung, D. H.; Bergman, R. G.; Raymond, K. N. *J. Am. Chem. Soc.* **2006**, *128*, 9781−9797.
(8) Yeh, R. M.; Raymond, K. N. *Inorg. Chem.* **2006**, *45*, 1130−1139.
(9) Wuerthner, F.; You, C.; Saha-Moeller, C.; Chantu, R. *Chem. Soc. Rev.* **2004**, *33*, 133−146.
(10) Evans, O. R.; Lin, W. *Acc. Chem. Res.* **2002**, *35*, 511−522.
(11) Holliday, B. J.; Mirkin, C. A. *Angew. Chem., Int. Ed.* **2001**, *40*, 2022−2043.
(12) Moulton, B.; Zaworotko, M. J. *Chem. Rev.* **2001**, *101*, 1629−1658.
(13) Caulder, D. L.; Raymond, K. N. *Acc. Chem. Res.* **1999**, *32* (11), 975−982.
(14) Cotton, F. A.; Lin, C.; Murillo, C. A. *Acc. Chem. Res.* **2001**, *34*, 759−771.
(15) Seidel, S. R.; Stang, P. J. *Acc. Chem. Res.* **2002**, *35*, 972−983.
(16) Linton, B.; Hamilton, A. D. *Chem. Rev.* **1997**, *97*, 1669−1680.
(17) Steel, P. J. *Acc. Chem. Res.* **2005**, *38*, 243−250.
(18) Eddaoudi, M.; Moler, D. B.; Li, H.; Chen, B.; Reineke, T. M.; O'Keeffe, M.; Yaghi, O. M. *Acc. Chem. Res.* **2001**, *34*, 319−330.
(19) Trofimenko, S. *Scorpionates: The Coordination Chemistry of Polypyrazolylborate Ligands*; Imperial College Press: London, 1999.
(20) Otero, A.; Antiñolo, J. F. B.; Tejeda, J.; Lara-Sánchez, A. *Dalton Trans.* **2004**, 1499−1510.
(21) Calhorda, M. J.; Costa, P. J.; Crespo, O.; Gimeno, C.; Jones, P. G.; Laguna, A.; Naranjo, N.; Quintal, S.; Shi, Y.; Villacampa, M. D. *Dalton Trans.* **2006**, 4104−4113.
(22) Reger, D. L.; Semeniuc, R. F.; Gardinier, J. R.; O'Neal, J.; Reinecke, B.; Smith, M. D. *Inorg. Chem.* **2006**, *45*, 4337−4339.
(23) Reger, D. L.; Semeniuc, R. F.; Little, C. A.; Smith, M. D. *Inorg. Chem.* **2006**, *45*, 7758−7769.

10.1021/ic062226u CCC: $37.00
Published on Web 02/08/2007

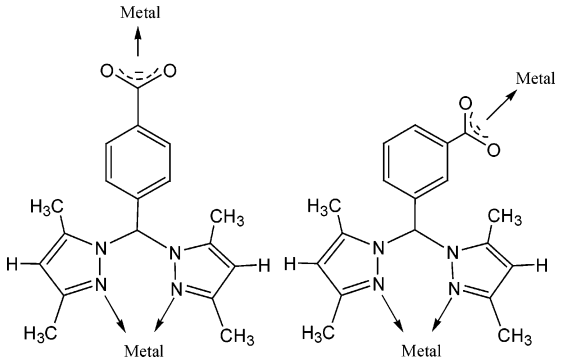

Here we redesign several heteroscorpionate ligands and explore their potential use as diatopic bridging units for the development of new supramolecular assemblies. To accomplish this, we have altered the position of the X functional group on the aromatic ring in the N_2X heteroscorpionate ligands so that they can no longer function as facially coordinating tridentate tripods but instead allow bridging interactions between metal nuclei. These new heteroscorpionates can thus be expected to function as binucleating ligands.[26] It is hoped that these binuclear blocks can, when combined with various linkers, produce unique and controllable supramolecular architectures. This paper is the first of a series of reports in which the full details of our work be presented. We report herein the preparation, synthesis, and characterization of five potential copper-containing building blocks and evaluate their ability to produce higher-order structures.

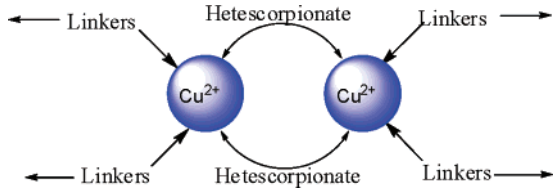

Experimental Section

Materials. All chemicals and solvents used during the syntheses were reagent grade. Bis(3,5-dimethylpyrazolyl)ketone was prepared according to the procedure described by Peterson et al.[27] ***Caution****: Perchlorate salts are dangerous (especially if they are dry) and should be handled with care.*

Ligand Synthesis. (4-Carboxyphenyl)bis(3,5-dimethylpyrazolyl)methane (L4c). Bis(3,5-dimethylpyrazolyl)ketone (2.4 g, 11 mmol) was placed in a 100 cm^3 round-bottomed flask. 4-Carboxybenzaldehyde (1.62 g, 10.8 mmol), $CoCl_2$ (20 mg), and triethylamine (4 mL) were then added. The mixture was heated to 120 °C for 4 h with vigorous stirring, during which the mixture turned deep purple and evolved CO_2. The flask was then allowed to cool to room temperature. The solid was taken up in water and filtered. The filtrate was neutralized with 6 M hydrochloric acid. At approximately pH 5.4, a white solid began to precipitate. This solid was collected by filtration, washed with water, and dried in vacuum. Yield: 71%. ^{1}H NMR (500 MHz, d-chloroform): δ 2.18 (s, 6H, CH_3), 2.238 (s, 6H, CH_3), 5.912 (s, 2H, PzH), 7.017 (d, 2H, J = 7.8 Hz, ArH), 7.753 (s, 1H, CH), 7.946 (d, 2H, J = 7.7 Hz, ArH). ^{13}C ($CDCl_3$): δ 168.99, 148.71, 141.40, 140.97, 130.64, 130.31, 127.22, 107.34, 73.92, 13.47, 11.56. FT-IR (KBr) ν /cm^{-1}: $\nu_{(OH)}$ 3448 (br, carboxylate), 2920, $\nu_{(C=O)}$ 1690 (carboxylic acid), $\nu_{(C=N)}$ 1560 (s, pyrazolyl), $\nu_{(C-O)}$ 1257, $\nu_{(Ar)}$ 753. mp: 173(1) °C.

(3-Carboxyphenyl)bis(3, 5-dimethylpyrazolyl)methane, L3c. This ligand was synthesized in a manner similar to that described for L4c using 3-carboxybenzaldehyde in place of the 4-carboxybenzaldehyde. The white solid began to precipitate at pH 4.6. Yield: 65%. ^{1}H NMR (500 MHz, ($(CD_3)_2SO$): δ 2.08 (s, 6H, CH_3), 2.12 (s, 6H, CH_3), 5.92 (s, 2H, PzH), 7.23 (d, 2H, J = 7.8 Hz, ArH), 7.50 (t, 1H, J = 7.7 Hz, ArH), 7.66 (s, 1H, ArH), 7.92 (d, 2H, J = 7.7 Hz, ArH). ^{13}C NMR: δ 166.97, 147.01, 140.24, 137.31, 131.75, 130.77, 129.07, 128.51, 128.27, 106.40, 71.78, 13.45, 10.94. FT-IR (KBr) ν/cm^{-1}: 3448, 2920, 1690, 1560, 1257, 753. mp: 206(1)°C.

Copper Complexes. $Cu_2(L4c)_2(H_2O)_2(ClO_4)_2$ (1). A methanol solution (10 mL) of ligand L4c (120 mg, 0.370 mmol) was added to an aqueous solution (10 mL) of $Cu(ClO_4)_2\cdot 6H_2O$ (137 mg 0.370 mmol) at room temperature, and the mixture was stirred for 2 h. The resulting green precipitate was collected by filtration, washed with methanol and water, and dried under vacuum for 2 h. Yield: 166 mg (0.164 mmol, 89%). Anal. Calcd (Found) for $[Cu_2(L4c)_2(H_2O)_2(ClO_4)_2]\cdot 2H_2O$, $C_{36}H_{46}Cl_2Cu_2N_8O_{16}$: C, 41.38 (41.45); H, 4.44 (4.06); N, 10.72 (11.32). IR (KBr) ν/cm^{-1}: 3415, 1558, 1487, 1436, 1109, 862, 769, 625. λ_{max}(CH_3CN): 734 nm. μ_{eff}: 2.84 μ_B (solid, 295 K). ESI-MS: *m*/*z*: 774, 873.

Single crystals suitable for X-ray analysis were prepared by the careful diffusion of a methanol solution of L4c containing sodium methoxide into an aqueous solution of $Cu(ClO_4)_2\cdot 6H_2O$.

$Cu_2(L4c)_2Cl_2$ (2). This complex was prepared in a manner analogous to that of **1** using $CuCl_2$ in place of the perchlorate. Yield: 425 mg (0.5 mmol 73%). Anal. Calcd (Found) for $[Cu_2(L4c)_2Cl_2]\cdot 3H_2O$, $C_{36}H_{44}Cl_2Cu_2N_8O_7$: C, 48.11 (48.07); H, 4.93 (4.55); N, 12.47 (12.98). IR (KBr) ν/cm^{-1}: 3448, 1560, 1502, 1436, 1253, 858, 835, 766, 714. μ_{eff}: 2.75 μ_B. ESI-MS: *m*/*z* (acetonitrile): 775, 810.

Single crystals suitable for X-ray analysis were prepared by the careful diffusion of a methanol solution of L4c containing sodium methoxide into aqueous solution of $CuCl_2$.

Cu(L4c)acac(H_2O) (3). A methanol solution (10 mL) of Cu(acac)$_2$ (570 mg 2.17 mmol) was added to a methanol solution (10 mL) of ligand L4c (706 mg, 2.17 mmol). The resulting dark green solution was allowed to stand, and crystals were obtained by slow evaporation. These were collected by filtration, washed with water and ether, and dried under vacuum for 1 h. Yield: 625 mg (1.24 mmol, 57%). Anal. Calcd (Found) for $[Cu(L4c)acac(H_2O)]\cdot 2H_2O$, $C_{23}H_{32}CuN_4O_7$: C, 51.15 (50.70); H, 5.97 (5.45); N, 10.37(10.55). IR (KBr) ν/cm^{-1}: 3416, 1592, 1552, 1519, 1373, 825, 770, 715. λ_{max} (CH_3CN, ϵ): 730 nm (63.0 M^{-1} cm^{-1}). μ_{eff}: 1.68 μ_B (solid 295 K).

Cu(L4c)Cl_2 (4). An acetonitrile solution (10 mL) of $CuCl_2$ (69.6 mg 0.52 mmol) was added to acetonitrile solution (10 mL) of ligand L4c (168 mg, 0.52 mmol) at room temperature, and the mxture was stirred for 1 h. The resulting light green solution was precipitated with diethyl ether. The bright yellow precipitate was collected by filtration, washed with ether, and dried under vacuum for 1 h. Yield: 122 mg (0.265 mmol, 51%). Anal. Calcd (Found) for $[Cu(L4c)Cl_2]H_2O$, $C_{18}H_{22}CuN_4O_3Cl_2$: C, 45.34 (45.00); H, 4.65 (4.64); N, 11.75 (12.06). IR (KBr) ν/cm^{-1}: 3448, 1717, 1560, 1459,

(24) Reger, D. L.; Semeniuc, R. F.; Pettinari, C.; Luna-Giles, F.; Smith, M. D. *Cryst. Growth Des.* **2006**, *6*, 1068−1070.
(25) Ward, M. D.; McCleverty, J. A.; Jeffery, J. C. *Coord. Chem. Rev.* **2001**, *222*, 251−272.
(26) Gavrilova, A. L.; Bosnich, B. *Chem. Rev.* **2004**, *104*, 349−384.
(27) The K. I.; Peterson, L. K. *Can. J. Chem.* **1973**, *51*, 422.

1259, 1108, 873, 814, 756. λ_{max} (CH_3CN, ϵ) 453 nm (785 M^{-1} cm^{-1}). μ_{eff}: 1.73 μ_B (solid 295 K).

Single crystals suitable for X-ray analysis were prepared by the careful diffusion of diethyl ether into an acetonitrile solution of the complex.

$Cu_2(L3c)_2(H_2O)_4(ClO_4)_2$ (5). A methanol solution (10 mL) of ligand L3c (510 mg, 1.57 mmol) was added to an aqueous solution (10 mL) of $Cu(ClO_4)_2 \cdot 6H_2O$ (582 mg, 1.57 mmol) at room temperature, and the mixture was stirred for 3 days. The resulting blue precipitate was collected by filtration, washed with methanol and water, and dried under vacuum for 2 h. Yield: 509 mg (0.48 mmol, 62%). Anal. Calcd (Found) for $[Cu_2(L3c)_2(H_2O)_4(ClO_4)_2] \cdot H_2O$, $C_{36}H_{52}Cl_2Cu_2N_8O_{19}$: C, 39.35 (39.30); H, 458 (4.83); N, 10.20 (10.34). IR (KBr) ν/cm^{-1}: 3425, 1561, 1467, 1396, 1120, 1090, 762, 695, 636. λ_{max}(CH_3CN, ϵ) 736 nm (176 M^{-1} cm^{-1}). μ_{eff}: 2.49 μ_B (solid, 295 K). ESI-MS (acetonitrile): *m*/*z* 775, 873.

Single crystals suitable for X-ray analysis were prepared by the careful diffusion of a methanol solution of L3c into a sodium methoxide-containing aqueous solution of $Cu(ClO_4)_2 \cdot 6H_2O$.

Physical Methods. Elemental analyses were performed on all compounds by Numega, San Diego, CA. All samples were dried in vacuo prior to analysis. ^1H and ^{13}C NMR spectra were collected on Varian 200, 300, or 500 MHz NMR spectrometers. Chemical shifts are reported in parts per million relative to an internal standard of TMS. IR spectra were recorded as KBr disks on a ThermoNicolet Nexus 670 FT-IR spectrometer and are reported in wavenumbers. Cyclic voltammetric experiments were conducted using a BAS Epsilon (Bioanalytical Systems Inc., West Lafayette, IN) voltammetric analyzer. All experiments were done under nitrogen at ambient temperature in solutions with 0.1 M tetrabutylammonium hexafluorophosphate as the supporting electrolyte. Cyclic voltammograms (CV) were obtained using a three-electrode system consisting of glassy carbon or Pt working, platinum wire auxiliary, and SCE reference electrodes. The ferrocinium/ferrocene couple was used to monitor the reference electrode and was observed at +0.442 V with $\Delta E_p = 75$ mV and $i_{pc}/i_{pa} = 1.0$ in acetonitrile under these conditions. IR compensation was applied before each CV was recorded. Electronic spectra were recorded using a Cary 50 UV−vis spectrophotometer. Room-temperature magnetic susceptibility measurements of the metal complexes were determined using a MSB-1 magnetic susceptibility balance manufactured by Johnson Matthey and calibrated with mercury(II) tetrathiocyanatocobaltate-(II) ($X_g = 16.44(8) \times 10^{-6}$ cm^3 g^{-1}). Diamagnetic corrections were taken from those reported by O'Connor.[28] Solution studies were carried out in Wilmad coaxial NMR tubes in either acetonitrile or methanol with TMS as the internal standard. Electrospray mass spectra (ESI-MS) were recorded on a Finnigan LCQ ion-trap mass spectrometer equipped with an ESI source (Finnigan MAT, San Jose, CA). A gateway PC with Navigator software version 1.2 (Finnigan Corp., 1995−1997) was used for data acquisition and plotting. Isotope distribution patterns were simulated using the program IsoPro 3.0.

X-ray Crystallography. Crystals of ligand L4c and L3c and complexes **1**−**5** were mounted either in capillaries for room-temperature data collection or with nylon loops and paratone oil (Hampton Research) and were placed in the cold stream for low-temperature collection on a Bruker X8 APEX CCD diffractometer. The structures were solved using direct methods or via the Patterson function, completed by subsequent difference Fourier syntheses, and refined by full-matrix least-squares procedures on F^2. All non-hydrogen atoms were refined with anisotropic displacement coefficients and treated as idealized contributions using a riding model except where noted. All software and sources of the scattering factors are contained in the SHELXTL 5.0 program library (G. Sheldrick, Siemens XRD, Madison, WI).

(28) O'Connor, C. J. *Prog. Inorg. Chem.* **1982**, *29*, 203.

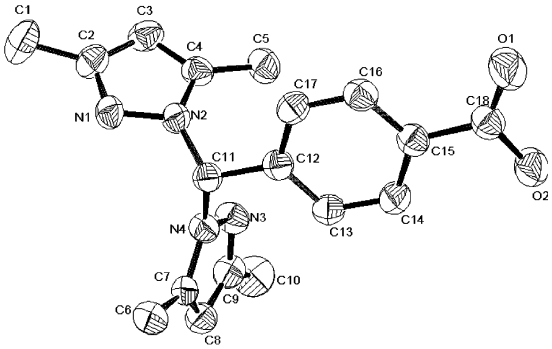

Figure 1. ORTEP diagram with 40% thermal ellipsoids of ligand L4c showing complete atomic labeling.

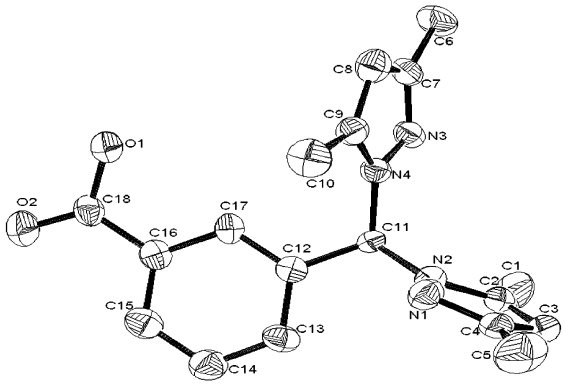

Figure 2. ORTEP diagram with 40% thermal ellipsoids of ligand L3c showing complete atomic labeling.

Results and Discussion

Synthesis and Characterization. Using our standard synthetic methodology, we placed the carboxyl donor group in a phenyl-substituted heteroscorpionate in a para or meta position and thus converted the ligand from a facially coordinating tripodal one favoring mononuclear complexes into one capable of bridging interactions. The structures of these two new ligands have been determined by X-ray crystallography and are shown in Figures 1 and 2. The reaction of the *p*-carboxylate ligand designated L4c in MeOH with aqueous solutions of the divalent metal Cu(II) leads to a head-to-tail 2M:2L dimer as the primary species as characterized by X-ray crystallography (vide infra). With copper perchlorate, the aquo complex is isolated, while the corresponding chloro derivative ensues starting with $CuCl_2$. Synthesis in nonaqueous solvents (methanol or acetonitrile) starting from $CuCl_2$ or $Cu(acac)_2$ as the metal source leads to mononuclear complexes **3** and **4**. In these cases, the carboxylate group of the heteroscorpionate remains uncoordinated, while the metal retains one or more of the anionic

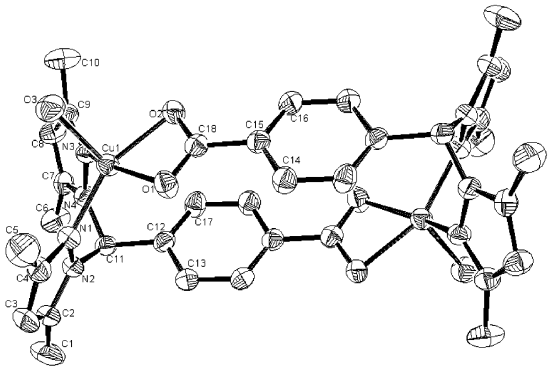

Figure 3. ORTEP diagram with 40% thermal ellipsoids of the cationic portion of $[(L4c)_2Cu_2\ (H_2O)_2](ClO_4)_2$ showing complete atomic labeling.

ligands present in the starting material. These reactions are summarized in the following graphic

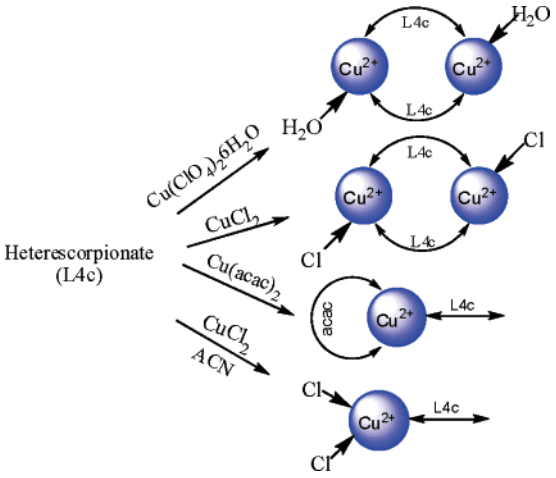

With the *m*-substituted ligand L3c, substantial changes in coordination about the copper ensue. In this case, sterics dictate that the carboxylate group coordinate in a unidentate rather than bidentate mode in the 2M:2L complexes so that the still pentacoordinate copper responds by picking up a second water molecule to complete the coordination sphere giving rise to a diaquo species.

Solid-State Chemistry. An ORTEP drawing of the cationic part of $Cu_2(L4c)_2(H_2O)_2(ClO_4)_2$ **(1)** is shown in Figure 3. The crystal structure reveals that the molecular entity possesses a crystallographic inversion center making only one-half of the dimer unique. In this complex, the two copper atoms are both five coordinate and can be described as having a distorted square pyramidal geometry, where the two nitrogen and two carboxylate oxygen donors of the chelating L4c ligands occupy the four positions of the basal plane, while one H_2O molecule is 2.202(2) Å away in the apical position. The intramolecular Cu−Cu distance is large (7.762 Å). The carboxylate groups are bound to the coppers in a regular bidentate mode with very similar Cu−O bonds of 2.013 and 2.035 Å. The average N_{pz}−Cu(1)−O(3) angle is 104°; both the N_{pz}−Cu(1)-O bond angles in the basal plane therefore deviate significantly from 90°. The N(3)−Cu(1)−N(1) angle is 90.59°, while the bidentate binding mode of the carboxylate constrains the O1−Cu(1)−O(3) angle to

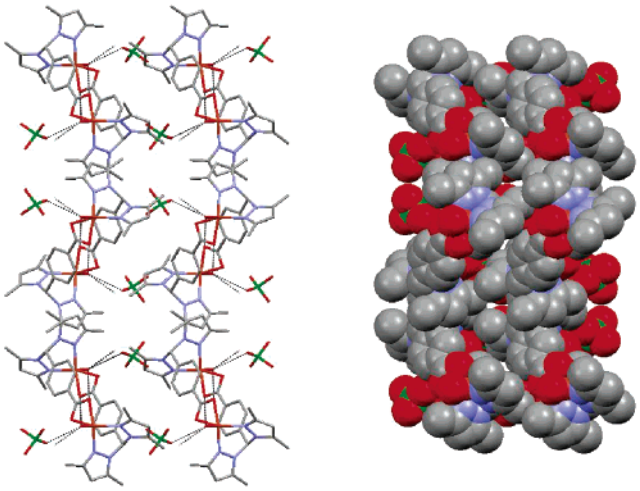

Figure 4. Crystal packing diagram for $[(L4c)_2Cu_2(H_2O)_2](ClO_4)_2$ as seen along the crystallographic *c* axis. Hydrogen bonds are shown as dotted lines.

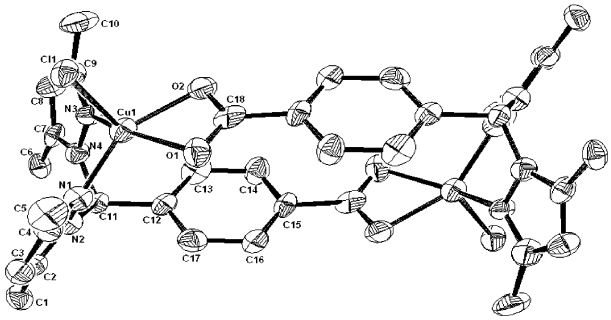

Figure 5. ORTEP diagram with 40% thermal ellipsoids of $[(L4c)_2Cu_2Cl_2]$ showing complete atomic labeling.

65.27°. The Cu atom sits 0.38 Å out of the mean N1, N3, O1, O3 plane. Because the complex is cationic, there is a slightly disordered perchlorate in the lattice that functions as a counterion and is involved in the hydrogen-bonding interactions that lead to extended structures in the crystal (Figure 4). The complex packs in extended columns because of H-bonding interactions between the ligand water molecules and the carboxylate groups on succesive dimeric units. H-bonding intereactions between the perchlorate ions and the water molecules serves to link the columns together.

The corresponding dinuclear complex $Cu_2(L4c)_2Cl_2$ **(2)** (Figure 5), prepared from $CuCl_2$ as a starting material, is extremely similar. Each copper is again pentacoordinate but with a chloride rather than a water as the axial ligand. In addition, the Cu is significantly further out of the basal plane, (0.45 vs 0.38 Å) than in the aquo complex. Otherwise, the bond lengths and angles are similar with the only notable difference being the 2.354 Å Cu−Cl distance that is expectedly larger than the $Cu-O_{water}$ distance. While there is no counterion in the lattice, a disordered methanol of crystallization is present whose H-bonding interactions drive the extended network seen in the crystal packing (data not shown).

On the other hand using methanol as a solvent, without any deliberately added water, and $Cu(acac)_2$ as a copper source, we isolate the mononuclear complex Cu(L4c)acac-(H_2O) **(3)** shown in Figure 6 which crystallizes in space

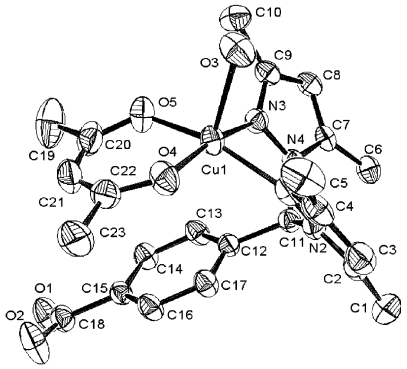

Figure 6. ORTEP diagram with 40% thermal ellipsoids of [(L4c)Cu(acac)-H_2O] showing complete atomic labeling.

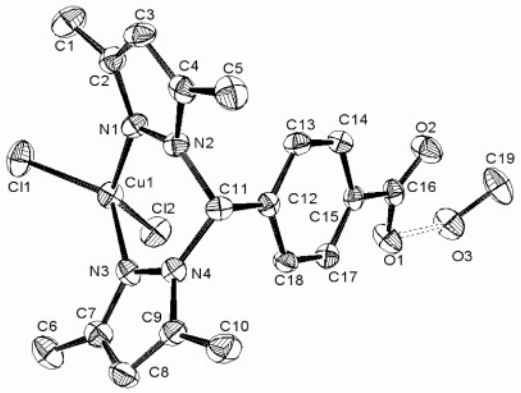

Figure 7. ORTEP diagram with 40% thermal ellipsoids of [(L4c)$CuCl_2$]·MeOH showing complete atomic labeling.

group *C*2/c. Structurally, the copper is again pentacoordinate in a square pyramidal geometry with the two pyrazole nitrogens and the two acetylacetonate oxygens now making up the basal plane with a water molecule occupying the axial position. Since there are no counterions in the structure, charge considerations indicate that either the coordinated "water" is actually a hydroxide or that the carboxylate group, which is uncoordinated, is deprotonated. The average 2.27 Å Cu−O distance clearly indicates a coordinated water and not a hydroxide ion; hence the carboxylate must be deprotonated and (surprisingly) uncoordinated. Other bond lengths and angles within the structure are unexceptional except that the Cu is closer to the basal plane (0.25 Å) than in the other two structures. A series of water molecules in the lattice provides hydrogen bond interactions that lead to extended structures within the crystal (data not shown).

The coordination environment around the copper in Cu-(L4c)Cl_2 **(4)** is considerably different than the pseudosquare pyramidal geometry seen in **1**−**3** (Figure 7). Thus, in **4**, the Cu is only four coordinate and is best described as distorted tetrahedral where the largest angular deviations from ideal are found for N1−Cu−Cl2 and N3−Cu−Cl1, which are near 132°. The remaining angles are all below the idealized 109° and average ∼99°. The twist angle between the Cl1−Cu1−Cl2 and N1−Cu1−N3 planes at 63.6° is much closer to the 90° angle expected of a tetrahedron, as compared to the 0° angle for the alternate square planar description. H-bonding between the lattice methanol, the chloride, and the protonated

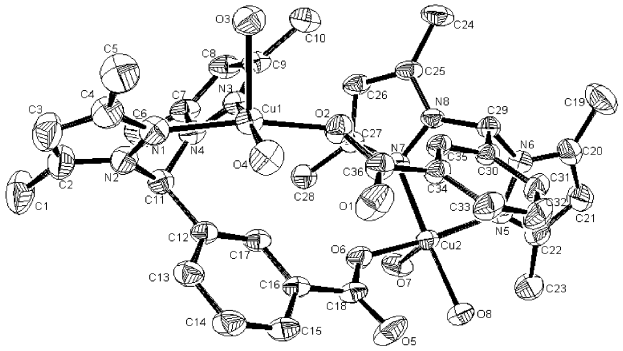

Figure 8. ORTEP diagram with 40% thermal ellipsoids of the cationic portion of $[(L3c)_2Cu_2(H_2O)_2](ClO_4)_2$ showing complete atomic labeling.

carboxyl group lead to a zigzag extended network in the solid state (data not shown).

When the *m*-substituted ligand, L3c, is used, a new dinuclear 2M:2L complex, $Cu_2(L3c)_2(H_2O)_4(ClO_4)_2$ **(5)**, is produced using copper perchlorate as the metal source. Here, the dinuclear unit does not possesses a crystallographic inversion center, and there are substantial changes in coordination about the copper as compared to the analogous complexes **1** and **2**. In **5**, steric considerations dictate that the carboxylate group coordinate in a unidentate rather than bidentate fashion ($Cu-O_{carboxylate}$ distances of 1.96 and 3.27 Å) so that the still pentacoordinate copper responds by picking up an additional water molecule to complete the coordination sphere (Figure 8). The geometry around each copper can still be described as distorted square pyramidal with one molecule of H_2O, two pyrazole nitrogens, and one carboxylate oxygen donor of the chelating L3c ligands occupying the four positions in the basal plane, while a second H_2O molecule sits in the apical position. The intramolecular Cu−Cu distance is near 6.8 Å, about an angstrom closer together than in the analogous *para*-carboxylate ligand complexes. The perchlorate ions and water molecules contribute H-bonding interactions that lead to a different packing and extended network structure than that seen for the complexes of L4c, as shown in Figure 9. Here the dinuclear units are stacked in columns held together by H-bonding between the water molecules and Cu ligands; $\pi-\pi$ stacking interactions also appear to be important. The resulting 1-D columns are in turn H-bonded via the perchlorate ions and lattice water molecules which interact with each other and the water ligands on the copper to produce an extended array.

Solution Chemistry. Although complexes **1**, **2**, and **5** are clearly dimeric in the solid state, the question is do such structures persist in solution? The positive-ion mode ESI mass spectrum in acetonitrile solution is shown for $[Cu_2(L4c)_2(H_2O)_4](ClO_4)_2$ in Figure 10. The highest-mass cluster corresponds to the cation $[Cu_2(L4c)_2(H_2O)_4(ClO_4)]^+$, as expected if the complex remains dinuclear. The calculated isotope pattern is also in agreement with this formulation. A second intense mass cluster occurs with a nominal mass of 775 amu which corresponds to $[Cu_2(L4c)_2]^+$, a dinuclear species, where presumably one of the Cu ions has been reduced from Cu(II) to Cu(I) during the ionization process.

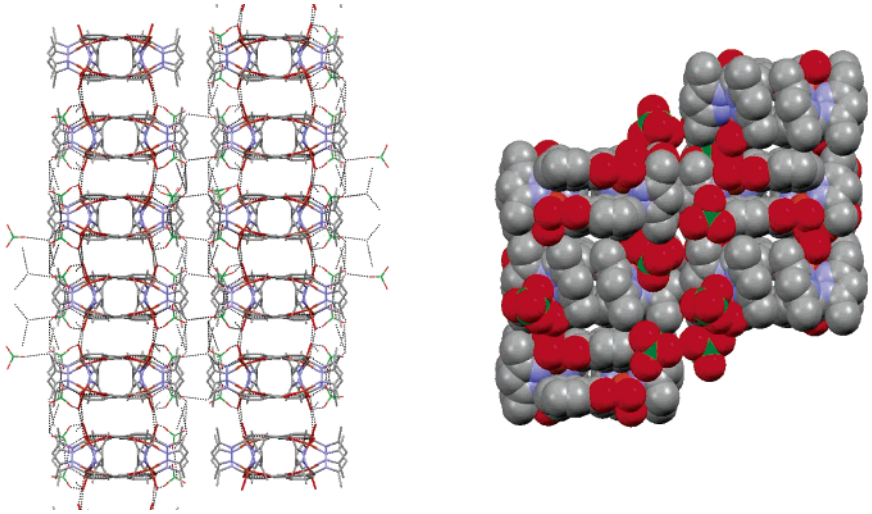

Figure 9. Crystal packing diagram for $[(L3c)_2Cu_2(H_2O)_2](ClO_4)_2$ as seen along the crystallographic *a* axis. Hydrogen bonds are shown as dotted lines.

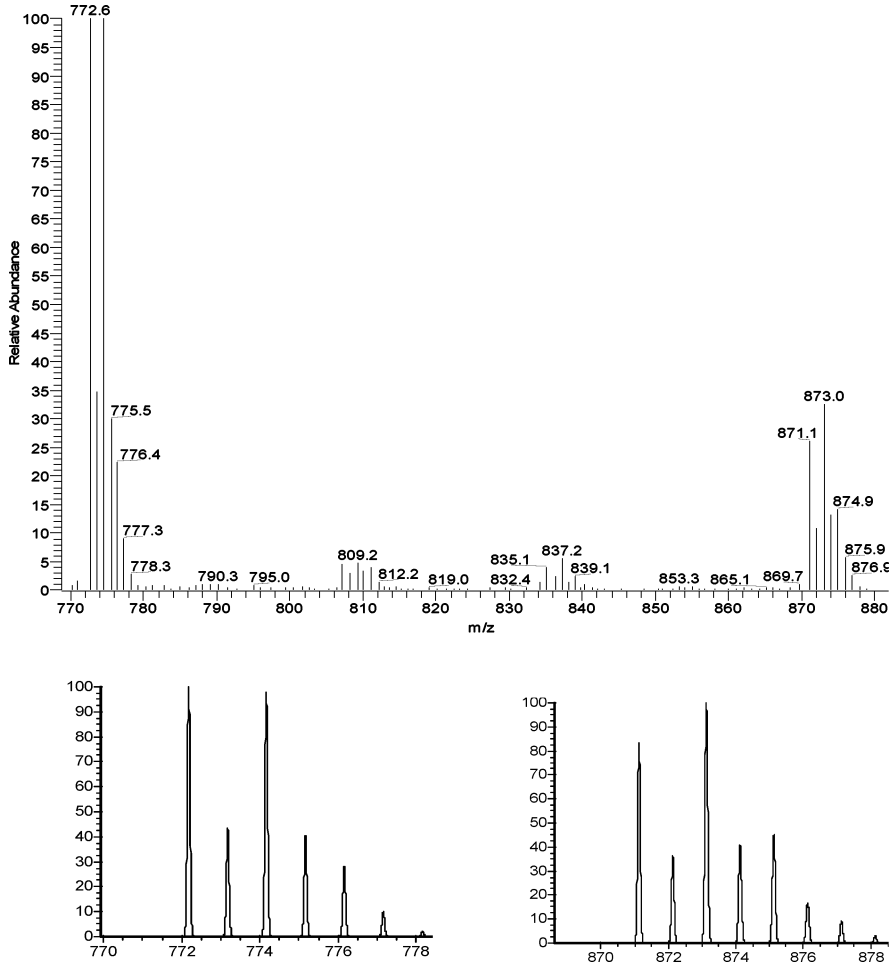

Figure 10. Positive-ion ESI-MS of $[(L4c)_2Cu_2(H_2O)_2](ClO_4)_2$ in acetonitrile. The upper frame shows the peak clusters associated with the $[(L4c)_2Cu_2(ClO_4)]^+$ ion (right) and the $[(L4c)_2Cu_2]^+$ ion (left). The lower frames show the calculated isotope distribution pattern expected for the fragments proposed.

The situation is different in methanol however (Figure 11) where the primary mass cluster at 711 amu corresponds to $[Cu(L4c)_2]^+$ indicating that the dimer has dissociated with loss of Cu to produce a mononuclear complex. Similar behavior is seen for **2** and **5**. That the apparent reductive events are the results of the electrospray ionization process and not indicative of the generic solution chemistry is shown by the magnetic susceptibility and electrochemistry results presented below.

Magnetic Measurements. Magnetic measurements gave values of near 2.8 μ_B for all the dimers in the solid state. This corresponds to moments near 1.79 μ_B/Cu indicative of simple nonmagnetically interacting d^9 Cu(II) ions. This is expected given the very long >6 Å through-space distance

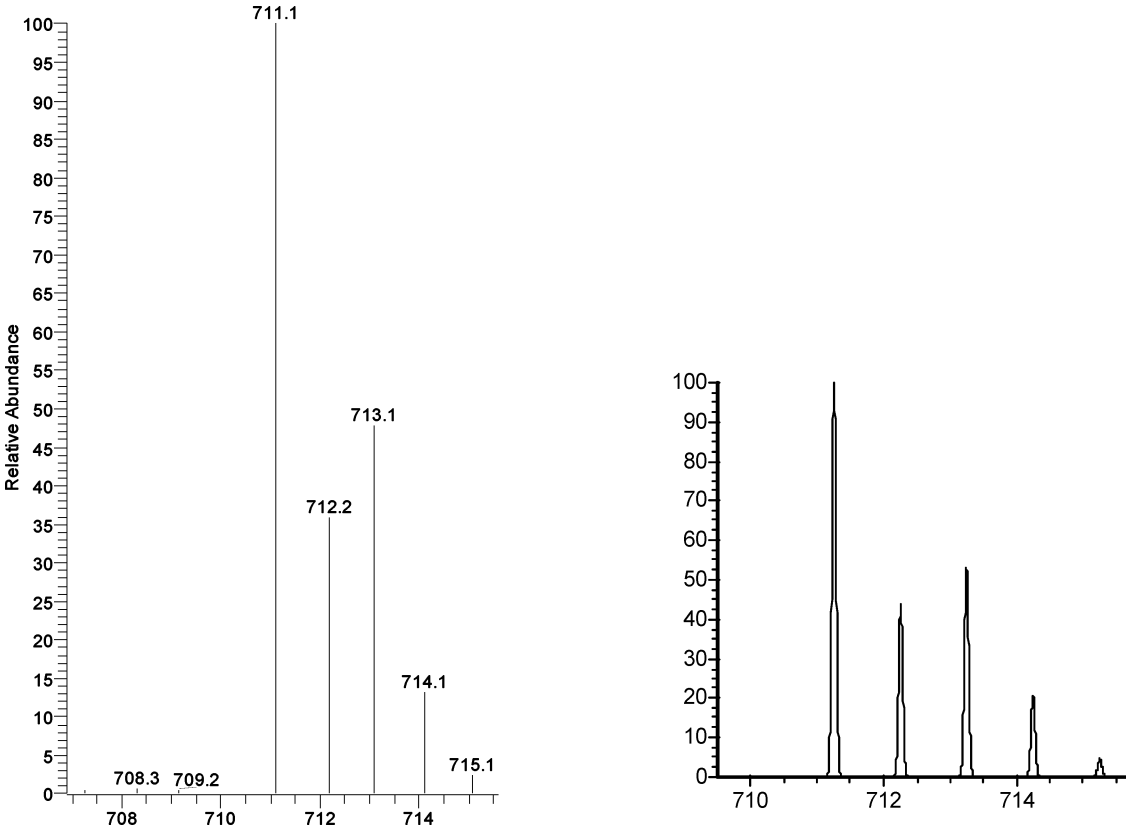

Figure 11. Positive-ion ESI-MS of $[(L4c)_2Cu_2(H_2O)_2](ClO_4)_2$ in methanol. The left panel shows the peak cluster associated with the $[(L4c)_2Cu]^+$ ion, while the right panel shows the calculated isotope distribution pattern expected for the fragment proposed.

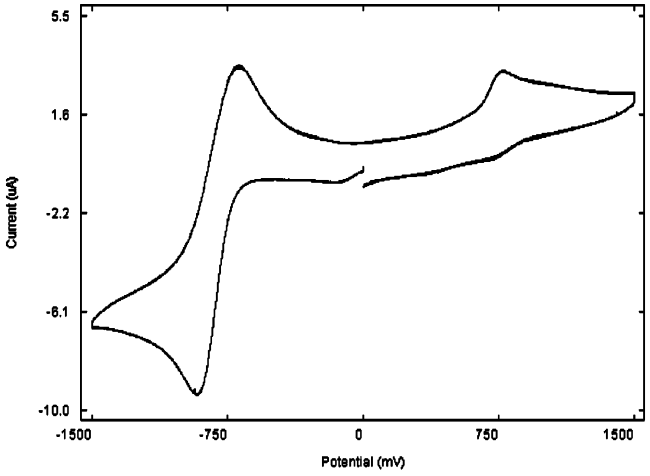

Figure 12. Cyclic voltammogram of $[(L3c)_2Cu_2(H_2O)_2](ClO_4)_2$ in acetonitrile at a scan rate of 100 mV s^{-1}.

between copper ions in the complexes. Virtually identical values are seen in solution as determined by the Evans method in either acetonitrile or methanol indicating that these complexes remain in the Cu(II) oxidation state in solution, but this unfortunately conveys no information about their nuclearity.

Electrochemical Properties. The electrochemical behavior of all the complexes were examined by cyclic voltammetry between 1.5 and −1.5V. The results are presented in Figure 12 and Table 4. The CV of **5** is representative of the dimers and shows a quasireversible wave at $E_{1/2} = -0.850$ V ($\Delta E_p = 0.231$ V, $\upsilon = 0.1$ V s^{-1}) and an irreversible oxidative wave near +0.6 V. Given the very long Cu−Cu distance and their non-interacting nature, this corresponds to a simple Cu(II)/Cu(I) couple on each copper. The change of the bridging ligand from L3c to L4c has little effect on the reduction potential but substantially reduces the reversibility of the couple suggesting that the latter complexes are more prone to dissociation in solution. Replacement of the axial water by a chloride has the expected effect of reducing the reduction potential by about 100 mV. The cyclic voltammogram of the mononuclear complex Cu(L4c)acac-(H_2O) looks very similar to that of the corresponding dimer, $[Cu_2(L4c)_2(H_2O)_4(ClO_4)]^+$, suggesting that the former may rearrange in solution to the latter. The electrochemical behavior of the mononuclear, pseudotetrahedral Cu(L4c)-Cl_2 is very different as a quasireversible oxidative (Cu(II)/Cu(III)), rather than reductive, wave is observed at +0.500 V with $\Delta E_p = 0.110$ V.

Conclusions

We have shown, by using our previously reported synthetic strategy, that we can transform heteroscorpionate ligands from tripodal-coordinating, mononuclear-favoring ligands into ones capable of bridging and producing dinuclear species. The dinuclear species appear to persist in solution in less polar solvents (e.g., acetonitrile) but to rearrange in more polar ones (e.g., methanol). Changing the position of the X group in these N_2X ligands produces subtle changes in the coordination environment around the copper in the dimers. Replacement of the labile water or halide ligands

Table 1. Summary of Crystallographic Data and Parameters for L4c, L3c, $[(L4c)_2Cu_2(H_2O)_2](ClO_4)_2$ (**1**), $[(L4c)_2Cu_2(H_2O)Cl_2]$ (**2**), $[(L4c)Cu(acac)(H_2O)]$ (**3**), $[(L4c)CuCl_2]\cdot MeOH$ (**4**), and $[(L3c)_2Cu_2(H_2O)_2](ClO_4)_2$ (**5**)

	L4c	L3c	1	2
molecular formula	$C_{18}H_{22}N_4O_2$	$C_{18}H_{19}N_4O_2$	$C_{18}H_{21}N_4O_{17}$-ClCu	$C_{18.5}H_{19}N_4O_{2.5}$-ClCu
fw	326.40	323.37	504.38	436.37
temp (K)	298(2)	200(2)	298(2)	200(2)
cryst syst	monoclinic	monoclinic	monoclinic	monoclinic
space group	$P2_1/c$	$P2_1/c$	$P2_1/c$	$P2_1/c$
cell constants				
a (Å)	10.1408(3)	12.7148(8)	9.2908(5)	9.300(3)
b (Å)	10.8961(3)	9.6352(7)	22.7790(12)	15.852(5)
c (Å)	16.3592(4)	13.8772(10)	10.0016(5)	13.942(6)
α (deg)	90	90	90	90
β (deg)	105.9460(10)	90.574	102.100(2)	107.607(10)
γ (deg)	90	90	90	90
Z	4	4	4	4
V (Å^3)	1738.06(8)	1700.0(2)	2069.66(19)	1959.0(13)
abs coeff, μ_{calcd} (mm^{-1})	0.084	0.085	1.234	1.275
μ_{calcd} (g/cm^3)	1.247	1.263	1.619	1.480
F(000)	696	684	1036	896
cryst dimensions (mm)	0.3 × 0.2 × 0.3	0.2 × 0.3 × 0.1	0.4 × 0.4 × 0.2	0.1 × 0.2 × 0.1
radiation	Mo Kα (λ =0.71073 Å)	Mo Kα (λ =0.7107 Å)	Mo Kα (λ =0.71073 Å)	Mo Kα (λ = 0.71073 Å)
h,k,l	−13 → 13, −14 → 14, −20 → 15	−13 → 13, −10 → 9, −14 → 13	−12 → 11, −28 → 30, −11 → 13	−11 → 10, −17 → 18, −16 → 16
θ range (deg)	2.13−27.54	2.57−22.41	2.27−28.95	2.57−25.05
reflns collected	18 016	20 576	21 847	14 850
unique reflns	3948	2193	5299	3456
params	221	217	332	253
data/params ratio	17.86	10.10	15.96	13.66
$R(F)^a$	0.0572	0.0534	0.0476	0.0873
$R_w(F^2)^b$	0.1709	0.1688	0.1259	0.1781
GOF^c	1.031	1.034	1.003	0.985
largest diff peak and hole (e/Å^3)	0.389 and −0.524	0.494 and −0.331	0.480 and −0.353	1.942 and −0.603

	3	4	5
molecular formula	$C_{23}H_{28}N_4O_8Cu$	$C_{19}H_{20}Cl_2CuN_4O_3$	$C_{37}H_{46}N_8O_{20}Cl_2Cu_2$
fw	552.03	486.83	1120.80
temp (K)	298(2)	240(2)	200(2)
cryst syst	monoclinic	monoclinic	monoclinic
space group	$C2/c$	$P2_1/n$	$P2_1/c$
cell constants			
a (Å)	24.4844(7)	11.635(3)	16.8155(8)
b (Å)	10.9463(3)	14.149(3)	15.5036(7)
c (Å)	19.7862(5)	12.908(3)	18.9048(8)
α (deg)	90	90	90
β (deg)	103.899(2)	93.928(10)	100.917(2)
γ (deg)	90	90	90
Z	8	4	4
V (Å^3)	5147.7(2)	2120.2(8)	4839.3(4)
abs coeff, μ_{calcd} (mm^{-1})	0.901	1.310	1.073
μ_{calcd} (g/cm^3)	1.425	1.525	1.538
F(000)	2296	996	2304
cryst dimensions (mm)	0.6 × 0.4 × 0.2	0.3 × 0.1 × 0.05	0.5 × 0.5 × 0.4
radiation	Mo Kα (λ = 0.71073 Å)	Mo Kα (λ = 0.71073 Å)	Mo Kα (λ = 0.71073 Å)
h,k,l	−30 → 30, −13 → 13, −24 → 24	−12 → 12, −11 → 14, −13 → 13	−26 → 26, −24 → 24, −27 → 29
θ range (deg)	2.21−26.67	2.70−21.77	2.30−34.32
reflns collected	51 021	18 306	118 048
unique reflns	5419	2490	20 214
params	329	266	678
data/params ratio	16.47	9.36	29.81
$R(F)^a$	0.0548	0.0392	0.0586
$R_w(F^2)^b$	0.1606	0.0929	0.1746
GOF^c	1.033	1.016	1.076
largest diff peak and hole (e/Å^3)	0.730 and −0.728	0.389 and −0.430	1.312 and −1.143

[a] $R = [\sum|\Delta F|/\sum|F_o|]$. [b] $R_w = [\sum w(\Delta F)^2/\sum wF_o^2]$. [c] Goodness of fit on F^2.

Table 2. Selected Bond Lengths (Å) and Angles (deg) for $[Cu_2(L4c)_2(H_2O)_2](ClO_4)_2$, $Cu_2(L4c)_2Cl_2$, and $[Cu_2(L3c)_2(H_2O)_4](ClO_4)_2$

	1	2	5
Cu(1)−O(1)	2.013(2)	2.037(6)	
Cu(1)−O(2)	2.035(2)	2.051(7)	1.9589(19)
Cu(1)−O(3)	2.202(2)		2.196(2)
Cu(1)−O(4)			1.9672(19)
Cu(1)−N(1)	1.989(3)	1.992(8)	2.018(2)
Cu(1)−N(3)	1.986(2)	1.983(7)	2.0056(19)
Cu(1)−Cl(1)		2.354(3)	
Cu(2)−N(5)			2.013(2)
Cu(2)−N(7)			1.9959(18)
Cu(2)−O(6)			1.961(2)
Cu(2)−O(7)			2.215(2)
N(1)−Cu(1)−O(1)	96.47(10)	97.5(3)	
N(1)−Cu(1)−O(2)	156.58(10)	150.9(3)	167.53(9)
N(1)−Cu(1)−O(3)	104.11(10)		93.67(9)
N(1)−Cu(1)−O(4)			92.54(9)
N(1)−Cu(1)−Cl(1)		104.6(2)	
N(3)−Cu(1)−N(1)	90.59(10)	90.4(3)	88.64(9)
N(3)−Cu(1)−O(1)	152.17(10)	150.5(3)	
N(3)−Cu(1)−O(2)	99.46(9)	96.7(3)	87.55(8)
N(3)−Cu(1)−O(3)	104.09(10)		95.91(8)
N(3)−Cu(1)−O(4)			169.09(9)
N(3)−Cu(1)−Cl(1)		104.0(2)	
O(1)−Cu(1)−O(2)	65.27(9)	63.7(3)	
O(1)−Cu(1)−O(3)	100.23(10)		
O(1)−Cu(1)−Cl(1)		101.4(2)	
O(2)−Cu(1)−O(3)	93.94(9)	31.3(3)	98.53(9)
O(2)−Cu(1)−O(4)			89.00(8)
O(2)−Cu(1)−Cl(1)		100.93(19)	
O(3)−Cu(1)−O(4)			94.84(9)

Table 3. Selected Bond Distances (Å) and Angles (deg) for $(L4c)Cu(acac)(H_2O)$ and $(L4c)CuCl_2$

	3	4
Cu(1)−N(1)	2.047(3)	2.009(4)
Cu(1)−N(3)	2.010(3)	1.969(4)
Cu(1)−O(5)	1.914(3)	
Cu(1)−O(4)	1.913(3)	
Cu(1)−O(3)	2.272(3)	
Cu(1)−Cl(1)		2.2000(2)
Cu(1)−Cl(2)		2.215(2)
O(3)−Cu(1)−O(4)	94.75(12)	
O(3)−Cu(1)−O(5)	100.48(14)	
O(3)−Cu(1)−N(3)	96.90(12)	
O(3)−Cu(1)−N(1)	96.13(12)	
O(4)−Cu(1)−N(3)	168.11(12)	
O(4)−Cu(1)−N(1)	88.66(12)	
O(4)−Cu(1)−O(5)	92.91(13)	
N(3)−Cu(1)−O(5)	87.28(12)	
N(3)−Cu(1)−N(1)	87.78(11)	91.72(16)
N(1)−Cu(1)−O(5)	163.12(13)	
N(1)−Cu(1)−Cl(1)		105.04(13)
N(1)−Cu(1)−Cl(2)		136.14(13)
N(3)−Cu(1)−Cl(1)		131.96(13)
N(3)−Cu(1)−Cl(2)		99.31(12)
Cl(1)−Cu(1)−Cl(2)		98.57(6)

Table 4. Electrochemical Properties of $[Cu_2(L4c)_2(H_2O)_2]^{2+}$, $Cu_2(L4c)_2Cl_2$ Cu(L4c)acac(H_2O), Cu(L4c)Cl_2 and $[Cu_2(L3c)_2(H_2O)_4]^{2+}$

complex	$E_{1/2}$ (V)	ΔE_p (mV)	i_c/i_a
(1) $[Cu_2(L4c)_2(H_2O)_2]^{2+}$	−0.895	326	0.80
(2) $Cu_2(L4c)_2Cl_2$	−0.787	340	0.76
(3) Cu(L4c)acac(H_2O)	−0.840	347	0.56
(4) Cu(L4c)Cl_2	+0.500	124	0.95
(5) $[Cu_2(L3c)_2(H_2O)_4]^{2+}$	−0.853	247	1.0

on the metal with another diatopic ligand such as terephthalic acid or 4,4′-bipyridine should allow for the linkage of these dinuclear building blocks into larger multidimensional

structures of different geometries. Indeed, we have shown that the labile water or halide ligands on various metal dimers can be substituted by various exogenous carboxylates. These results will be presented in the future.

Acknowledgment. This work was supported in part by NSF Grant CHE-0313865. The NSF-MRI program Grant CHE-0320848 is also gratefully acknowledged for support of the X-ray diffraction facilities at San Diego State University.

Supporting Information Available: Additional crystallographic data (CIF files) for ligands L4c and L3c and complexes **1**−**5**. This material is available free of charge via the Internet at http://pubs.acs.org.

IC062226U